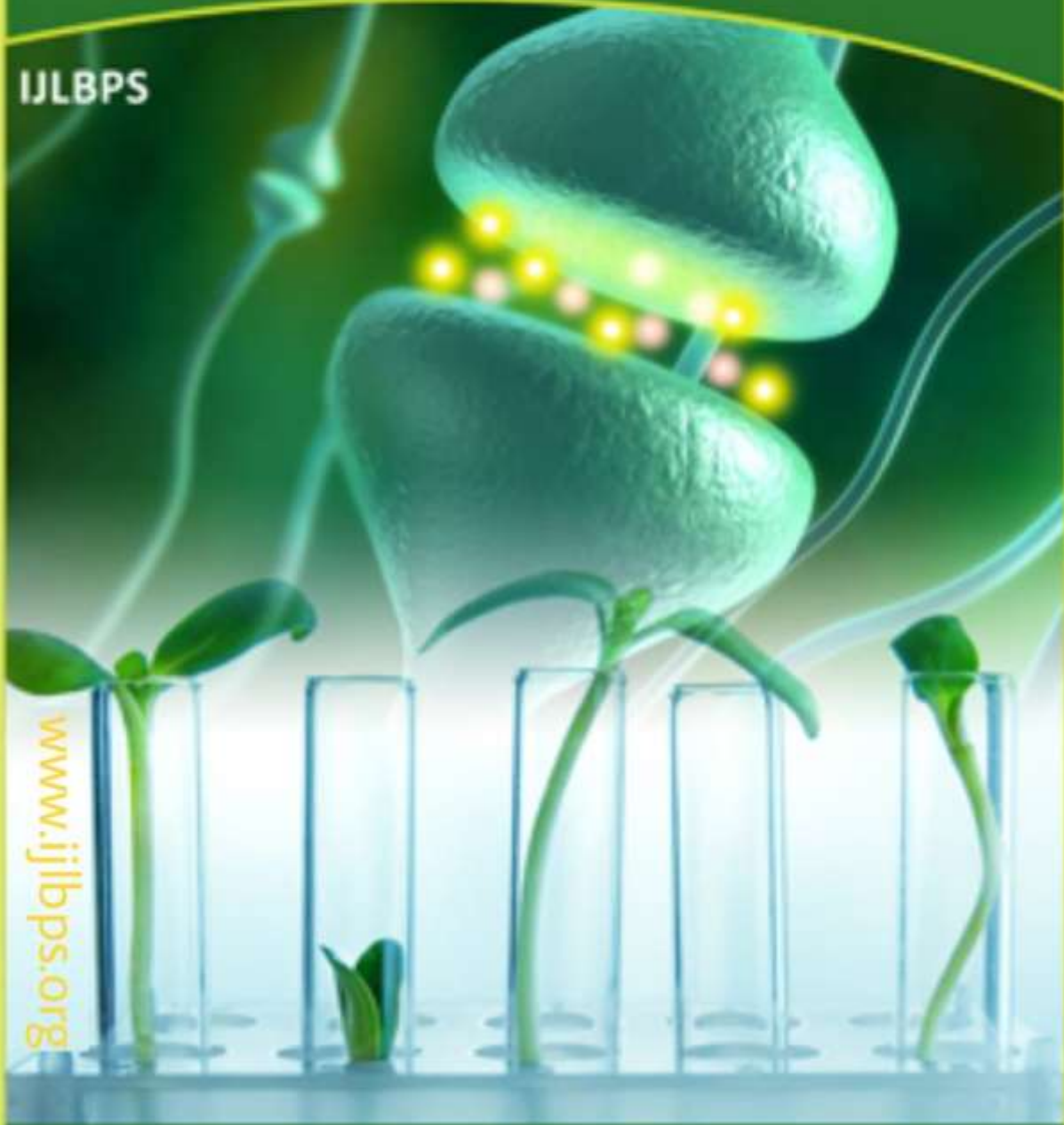




ISSN 2395-650X

International Journal of
Life Sciences Biotechnology Pharma Sciences

IJLBPS



www.ijlbps.org

E-mail: editorijlbps@gmail.com editor@ijlbps.org

Real-time Simulations on High-Performance Z-Source PV-Grid-Tied Inverters with DC Charger for EV Applications

1P.VenkataPraveenKumar,2K.SureshKumar

1PGScholar, 2Associateprofessor

1,2Department of Electrical and Electronics Engineering, Dr. Samuel Georgeinstituteof engineering and technology, Prakasam, A. P, India

1pravinkumar261996@gmail.com,2spandu625@gmail.com

Abstract

Solar power is the most prevalent green energy source for household and semi-commercial applications. Using energy storage devices, fluctuations in solar energy collecting can be reduced (ESS). Solar electricity can also be utilized to charge electric vehicle batteries, reducing reliance on the grid. To qualify as such converters, they must have a limited number of steps and a separation. It is possible to eliminate multiple stages of conversion by using the Z-source inverter (ZSI) topology. The use of passive materials allows for the incorporation of ESS. To charge the batteries of electric vehicles using direct current, this article describes the design, building, and operation of a modified ZSI equipped with a split primary separated battery charger. Simulated results have been used to demonstrate the feasibility of the proposed converter's operation.

Keywords: SRM, Inverter, EV, and speed/load.

1. Introduction

Currently, the AC grid is frequently utilized for charging electric vehicles. Regardless of how effective the topology is, various charging techniques that only use an AC grid, such as wireless charging or plug-in charging, can still generate pollution. While charging an electric vehicle, it's important to know how much fossil fuels are used to generate the electricity needed. Renewable energy sources can be integrated into charging infrastructure to lessen the need for electricity from the main grid [1]. Isolation transformers in converter topologies enable galvanic isolation at the user end of the high-voltage system in order

to give safety measures when creating an EV battery charger. It is possible to achieve galvanic separation on either the charger or the ac grid side [2]. On the grid side, isolation transformers tend to be significantly larger than those on the charging side. High-frequency switching has made it possible to employ smaller transformers for galvanic separation because of improvements in semiconductor technology [3].

It has been utilized in the past for commercial charging infrastructure with photovoltaic (PV) grid connection systems They reduce the need for an AC power grid to supply charging infrastructure. Residential charging systems

for electric vehicles (EVs) can benefit from using solar and grid-connected systems [4]. Single-phase inverters with a power output of up to 10 kW can be used in residential settings. There are a variety of isolated and non-isolated topologies with many stages available for connecting residential solar PV to the grid. For EV charging, residential PV systems need features such as isolation and voltage boosting capabilities to match the solar PV array voltage to the grid voltage needs [5]. [5]

Single-stage bucking or boosting and inversion of the input dc voltage are all possible. A lot of

attention has been paid to PV-grid-connected systems. An inverter based on Z-Source(ZSI) topology uses two capacitors and two inductors to boost the input dc voltage to match the inverter-side ac output voltage requirements. The operation of a ZSI is heavily dependent on the passive components [6]. It presents an opportunity to integrate energy storage units into such a system. In this project, a proof of concept of a single-phase Modified Z-Source Inverter (MZSI) based solar grid-connected charger has been presented as an application towards a string inverter configuration.

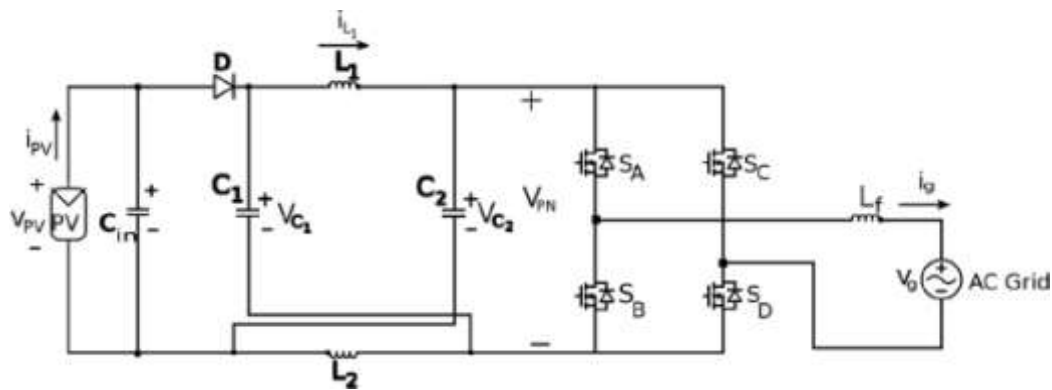


Figure 1. Schematic of a PV/ac Grid Interconnected ZSI

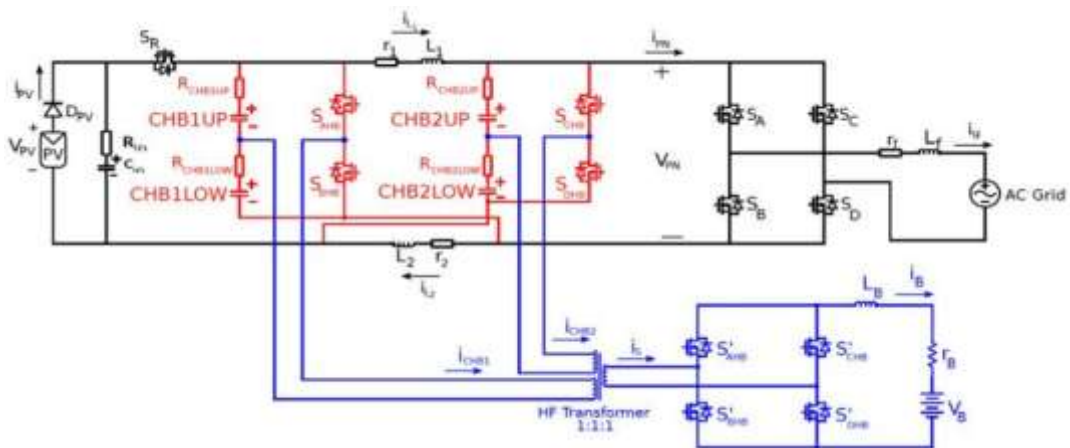


Figure 2. Detailed Schematic of the Proposed MZSI

1.2 Literature Survey

This work by D. Aggeler et al. [7] focuses on newly developed PE infrastructure technologies that enable quick battery charging operations. Now more than ever, Power Electronics (PE) is finding its way into several technical fields. One of these is electric mobility. Energy distribution for charging and energy transformation on board of the traction-related vehicles are just two examples of how Power Electronics presents itself as an emerging technology for improving sustainable mobility. In less than 10 minutes, depending on the battery and vehicle, a charge adequate for a trip distance of over 100 kilometers can be obtained [8]. It's only a matter of time before battery charging is as quick and easy as filling up at a gas station right now. On the basis of low- and high-frequency isolation requirements, two PE converter topologies for charging infrastructure applications are described and explored. The pros and cons of each of the two technologies will be discussed, as well as the advantages and disadvantages of each. Studying the grid's effect is done by means of simulation with the assumption of a dc fast charging station placed in a rural area in Sweden.

G. Carli and S. S. Williamson [9], analyzes one specific type of renewable, local energy generation, applied to electric vehicle charging requirements. It is now clear that the transportation sector will increasingly rely on electricity and the related infrastructure needed for storage and distribution. At the same time, the source of electricity itself must not be carbon based.

Rather, whenever possible, it should depend on environmentally responsible processes. In addition to their ecological benefits, aeolic and photovoltaic (PV) sources are highly scalable, and can be utilized for local generation and delivery, eliminating those energy losses normally associated with long-range grid distribution. A PV source is explicitly posited, because solar panels can be placed above the vehicle parking space, and double as a shade provider. In the first part of this paper, the optimal requirements for overall system are derived. These will be used in the second part, in the purpose of comparing various power conditioning circuits

[10] discusses the construction of a discrete event simulation framework that emulating the interactions between the power grid and plug-in hybrid electric vehicles and investigates if existing capacity can fulfill the PHEV load requirement of the current power system. Statistical transportation data is used to extract the probability distribution functions for each vehicle's arrival time and energy use. The inadequate generating and transmission capabilities of the electric system are seen as the key limitations. Because of this, vehicles may have to wait for a charge to arrive. Two real-world examples in the United States are used to demonstrate the validity of the suggested simulation framework, which is detailed in depth. We're thinking about both Level-1 and Level-2 charging options. Problem Formulation

If the dc-rail voltage exceeds the ac-input voltage, the ac output voltage is capped below the dc-rail voltage. That is why an

inverter for the voltage source converts voltage from one form to another: from one form to the other, the inverter acts as a boost (step-up) rectifier and the voltage source converter acts as an ac-to-dc inverter. When a higher ac output voltage is required but the existing dc voltage is insufficient, a second dc-dc boost converter is required. Cost and efficiency are lowered by an additional power converter stage.

For each phase leg, there is no way to turn on both the upper and lower devices at the same time. Otherwise, the devices would be destroyed by a shoot-through. One of the biggest threats to a converter's dependability is the misgating-on shootthrough problem caused by EMI noise. The voltage source converter must provide dead time to block both upper and lower devices, resulting in waveform distortion and other problems. A current-source inverter cannot produce a sinusoidal voltage without the use of an output LC filter, which results in increased power loss and management complexity.

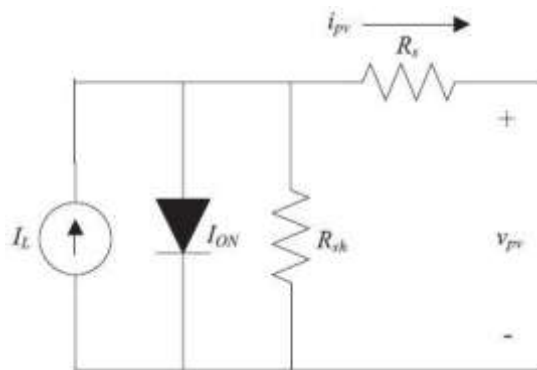
The dc voltage produced by the dc inductor is always smaller than the ac input voltage

2. Formatting your Paper

3. To put it another way, a photovoltaic (PV) cell is nothing more than a p-n junction diode.

because the ac output voltage must be greater than the original dc voltage that feeds the dc inductor. There is a buck converter (or current source rectifier) and a boost converter (or current source inverter) for dc-to-dc power conversion in the current source inverter. Additional dc-dc buck (or boost) converters are required for applications that require a large voltage range. Cost and efficiency are both impacted by an additional power conversion stage. In order to use high-speed and high-performance transistors like insulated gate bipolar transistors, the main switches of the current source converter must prevent reverse voltage (IGBTs). To avoid direct usage of low cost and high-performance IGBT modules and intelligent power modules (IPMs).

This paper presents an impedance-source (or impedance-fed) power converter (abbreviated as Z-source converter) and its control method for implementing dc-to-ac, ac-to-dc, ac-to-ac, and dc-to-dc power conversion in order to overcome the above problems of traditional voltage source and current source converters.



There is a simple equivalent circuit schematic of a PV cell in Figure 3. PV cell generated current is represented by a current source, which is in parallel with a diode and shunt and series resistances.

Figure 3 Equivalent circuit diagram of the PV cell

4. DC-DC Converters

DC-DC converter having a high step-up voltage that can be utilized in a variety of applications, including automotive headlights, fuel cell energy conversion systems, solar cell energy conversion systems, and uninterruptible power supply battery backup systems. Theoretically, a high effective duty ratio dc-dc boost converter can achieve a high step-up voltage. The step-up voltage gain is limited in practice by the influence of power switches and the ESR of inductors and capacitors, though.

To get a high step-up voltage gain with a high duty ratio, a traditional boost converter is typically employed. However, the losses of power switches and diodes, the equivalent series resistance of inductors and capacitors, and the reverse recovery difficulty of diodes limit the efficiency and voltage gain. In these converters, considerable voltage stress and power dissipation are caused by the active switch because of the transformer's leakage inductance. It is possible to decrease the voltage surge by using a resistor-capacitor-diode snubbed combination. However, this results in a decrease in effectiveness. Converters with low input ripple current are generated using a connected inductor. An extra LC circuit with a connected inductor is

used to achieve reduced input current ripple in these converters.

5. Inverter

Direct current (DC) can be converted to alternating current (AC) using proper transformers, switching, and control circuits, and the AC can be at any desired voltage and frequency. Small computer power supply to huge electric utility high voltage direct current applications can all benefit from using static inverters, which have no moving components and are employed in a wide range of applications. To convert DC electricity into AC power, inverters are often employed. Such as solar panels or batteries. The electrical inverter is a high power electronic oscillator. It is so named because early mechanical AC to DC converters made to work in reverse, and thus "inverted", to convert DC to AC.

4.1 Cascaded H-Bridges Inverter

Figure 4 depicts the single-phase structure of a cascaded inverter. A single phase full bridge inverter, often known as an H-bridge, is used to connect each individual DC source (SDCS). There are three alternative voltage outputs for each inverter level that can be generated by connecting the DC source to the DCdc ac output in different ways. four S1, S2, S3, and S4 are the on/off switches. Switches dc S1 and S4 are used to produce +Vdc, whereas S1 and S3 are used to produce -Vdc. The output voltage is 0 when S1 and S2 or S3 and S4 are turned on. These inverters are connected in series to produce a voltage waveform that is the sum of their AC outputs, which can be used to control other devices. In a cascade inverter, the number of output phase voltage

levels m is specified as $m = 2s+1$, where s is the number of distinct DC sources. For an 11-level H-bridge inverter with five SDCSs and five complete bridges, a phase voltage waveform is illustrated in Figure 5. The voltage across each phase + ... (1)

For stepped waveforms such as the one depicted in Figure 5 with s steps, the Fourier Transform for the waveform follows

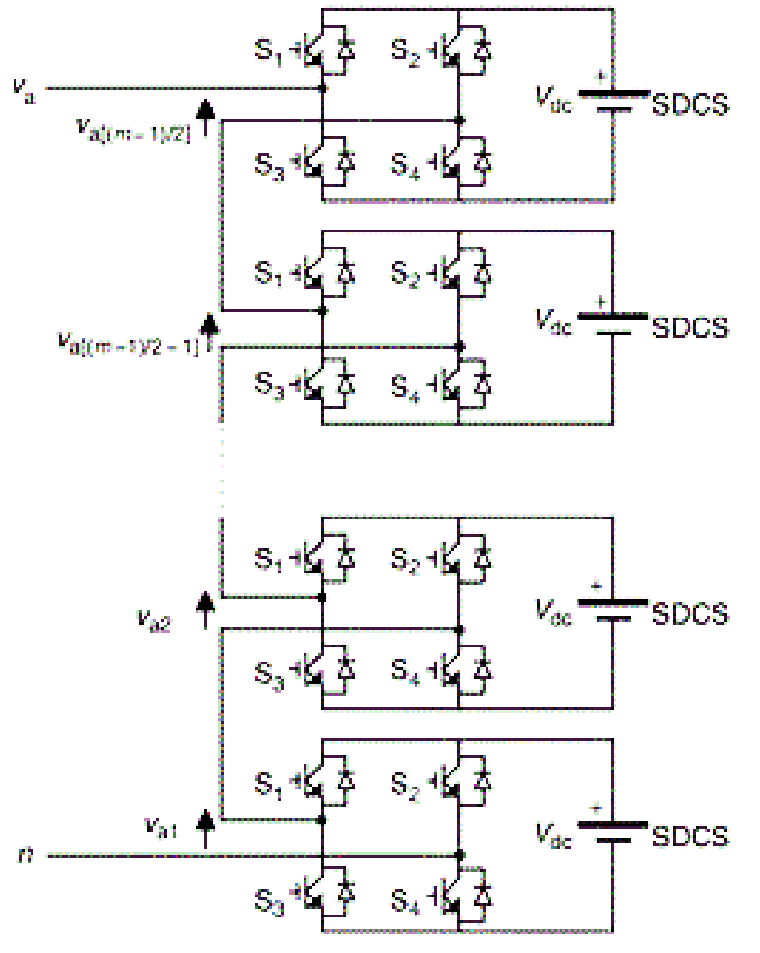


Figure 4. Single-phase structure of a multilevel cascaded H-bridges inverter

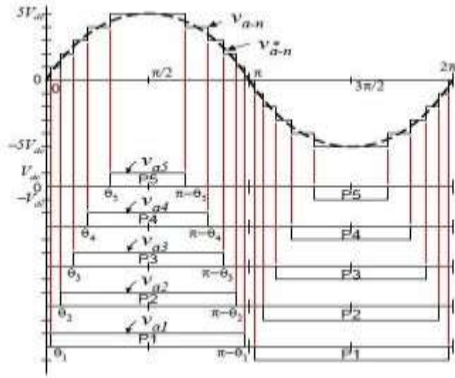


Figure 5 Output phase voltage waveform of an 11 level cascade inverter with 5 separate DC sources

6. Project Description and Control Design

5.1 Traditional ZSI

5.2 Figure 7 depicts the ZSI structure in two operational modes: shoot-through and non-shoot-through. $V_C = V_{C1} = V_{C2}$ is the formula for symmetrical operations. In the shoot-through mode, all four switches are engaged.

At the same time, SA, SB, SC, and SD are conducting. The duty cycle D_0 and switching frequency F_0 are used to characterize the length of this shoot-through state (FSW). A modified pulse width modulation (PWM) approach can be used to implement the shoot-through condition. As a result, the voltages between the two capacitors are written as

$$V_C = (1 - D_0)/(1 - 2D_0) v_{pv} \quad (3)$$

It can be shown that $Mv_{pv}/(1 - 2D_0)$ is equivalent to V_{grms} (7)

Using the VPN's peak dc-link voltage,

$$VPN \text{ is defined as } 1/(12D_0)v_{pv} \quad (4)$$

$I_{grms}V_{grms}$ is the power balance equation between the ac and dc sides of the ZSI (5)

The maximum dc-link current and voltage are denoted by IPN and VPN , respectively. The ZSI's maximum ac output voltage is

$$V_g \text{ is equal to } MVPN \quad (6)$$

V_g is the grid voltage modulation index.

For grid-connected applications, the grid current $i_g = I_g \sin(\omega t + \phi)$ for $\phi = 0$. The ZSI's output ac voltage's RMS value can be calculated from (11) and (13).

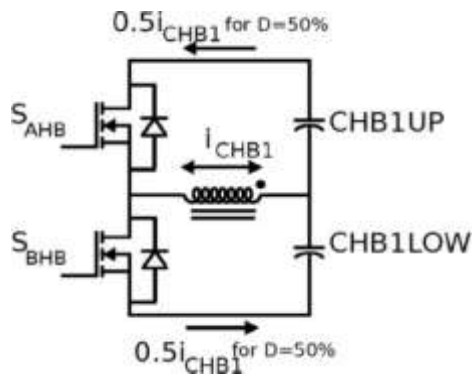


Figure 6. Schematic of one the primary across CHB1 operating at 50% duty cycle

5.23

Component Sizing, Modeling, and Control of the Proposed MZSI

MZSIs with integrated battery chargers are depicted in Figure 7. A split primary isolated half-bridge bidirectional operation of the MZSI is achieved by splitting the two capacitors (C1 and C2) from Figure 6, with each serving as one leg. To prevent the reverse flow of current back into PV, the diode DPV is used. Cin's input capacitor Rin has an internal resistance of Rin. Proposals have been made for the integration of the charger within the ZSI using a split primary dc-to-dc converter. One complete bridge secondary is isolated from a pair of HBC primaries using a high-frequency transformer. In an open loop, the HBC primary and secondary processors run at 50% duty cycle. The secondary's output current is routed to a power source, such as a lithium-ion battery. Since the HBC primary input voltages VC and vB are clamped together at the energy storage unit's input,

Each of the split primaries alternates between charging and providing half of the battery current. It is connected across the capacitors of each leg of the dc-dc converter's primary. The voltage applied across the capacitors is given by the expression: (15). In the simplified equivalent model shown in Figure 7, each of the two primary can be represented by an RLE circuit linked in series with the capacitors C1 and C2. As shown in Figure 7, the Kirchhoff's voltage law (KVL) equation can be applied to the modeled MZSI in the non-shoot-through state. $L \frac{di_L}{dt} = v_{pv} - i_L r + R_{HB} + (2i_g + i_B/2) R_{HB} - V_C$ (12) The Kirchhoff's current law (KCL) equation is

$$C \frac{dV_C}{dt} = i_L - i_g - i_B/4 \quad \text{.....(13)}$$

During the shoot-through state, the KVL equation is

$$L \frac{di_L}{dt} = V_C - i_L (R_{HB} + r) - (i_B/2) R_{HB} \quad \text{.....(14)}$$

The KCL equation is written as

$$C \frac{dV_C}{dt} = -i_L - i_B/4 \quad \text{.....(15)}$$

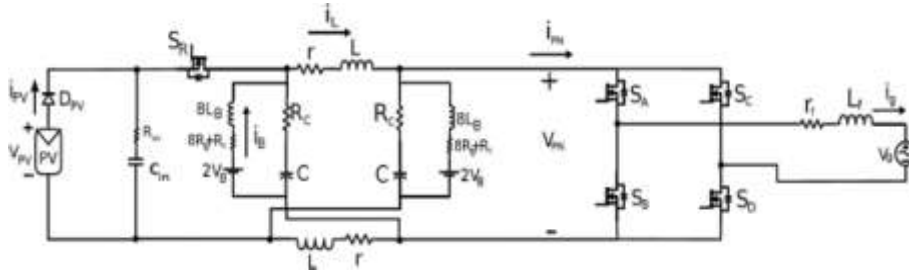


Figure 7. Equivalent model of the proposed MZSI with a battery

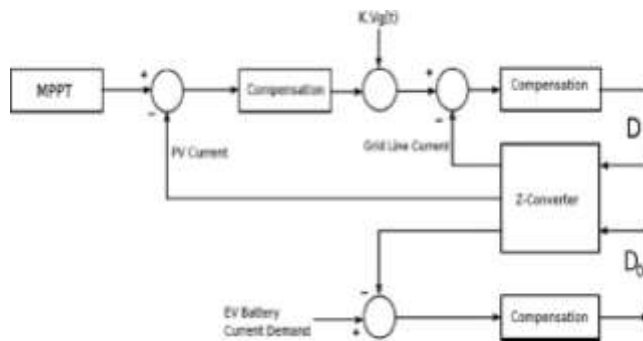


Figure 8. Block diagram of the control scheme of the proposed MZSI charger

5.24 Figure 7 depicts the battery current i_b and the grid ac current i_g flowing in the right direction. Figure 8 depicts the controller block diagram for the proposed MZSI topology

controller. The PV current i_{pv} loop, the grid current i_g loop, and the battery current i_b loop make up this system's three loops. H-bridge inverter output current or shoot-

through duty ratio D_0 is generated by controlling the voltage of the ZSI capacitor. By adjusting the maximum input PV current, a reference current is generated. In this case, the shoot-through duty ratio D_0 is dependent on the stiff voltage V_C applied across one or both capacitors. Battery loop control is slower

than input current control because the battery current loop does not require rapid dynamic changes. For the control of the battery loop.

5.25

Energy Management Scheme for the Proposed Converter

Block schematic of the proposed system shown in Figure 8. ZSIs that include an energy storage system (ESS) alter the formula (5) as follows: $V_{bib} + I_{grms}v_{grms}$ (18) where I_b and v_b are the battery current and voltage, respectively. A constant charging power P_B is obtained at the ESS due to the single-phase ac grid power P_g balancing the power fluctuations of the PV source P_{pv} . When pulling power from the grid to charge an EV battery, the direction of the ac grid current flow switches from positive to negative. The charger is powered by PV and the grid, which means that the inverter may run in both directions and keep the system in a power-balanced state.

the sum of the parts $V_{PV} + i_{grms}v_{grms} = v_{bib}$.. (19)

A grid-connected rectifier/charger can be used in the absence of PV if the voltage across the input capacitor C_{in} is maintained at the minimum value of the PV voltage.

7. Simulation Results

The simulation studies to demonstrate the behavior of the proposed topology have been carried out using PLECS 4 for a 3.3 kW charger for a string inverter configuration. Simulation has been carried out for the system shown in Figure 9, which shows that at a simulation time $t = 1.75$ s, the input PV power reduces from 2.8 to 2 kW and the grid power increases from 710 to 1500

W to maintain the output charger power to 3.3 kW.

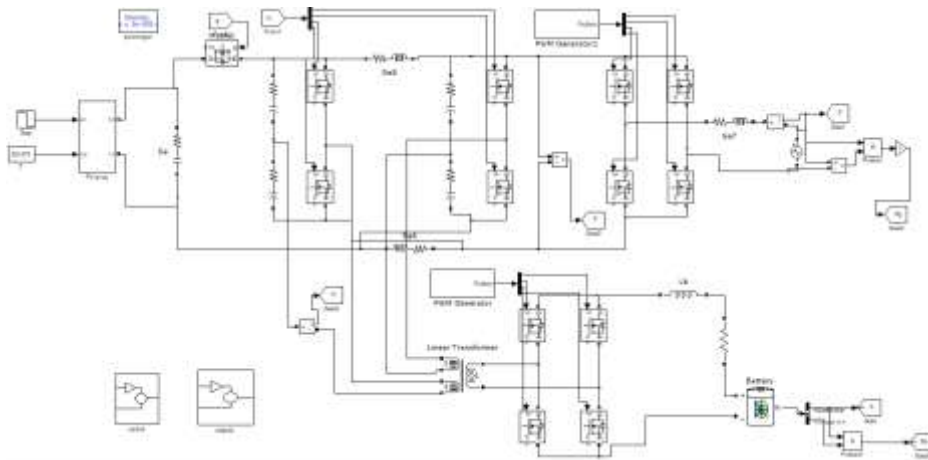


Figure 9. Overall Simulink diagram

Table 1. MZSI-Based Charger System Simulation Specifications

S.No	Parameters Value	Value
1	Input voltage, V_{in}	286V
2	Input current, I_{in}	9.8A
3	Inductor value, $L1=L2$	500 μ H
4	ZSI switching frequency, FSW	25kHz
5	Grid voltage (RMS), V_g	240V
6	Inverter output filter inductor, L_f	7.5mH

7	PVinputpower,PPV	2.8kW
8	Inputcapacitor,Cin	2mF
9	HBCoutputfilter,LB	1mH
10	HBCoutputfilter,LB	1mH
11	Batterychargepower,PB	3.3 kW

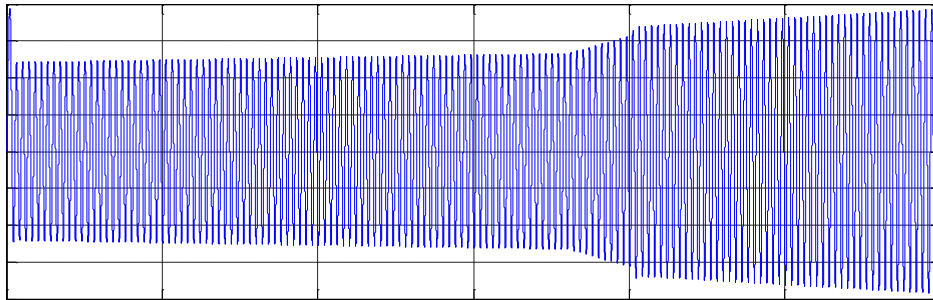


Figure10.OutputwaveformofGridcurrent

The above figure shows output waveform of grid current. In

his X-axis represents time in seconds and Y-axis represents grid current in amperes.

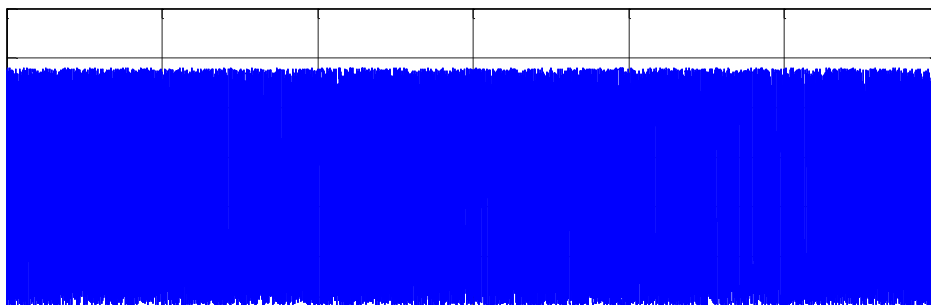


Figure11.OutputwaveformofDClinkvoltage

The above figure shows output waveform of DC link voltage. In this X-axis represents time in seconds and Y-axis represents DC link voltage in volts.

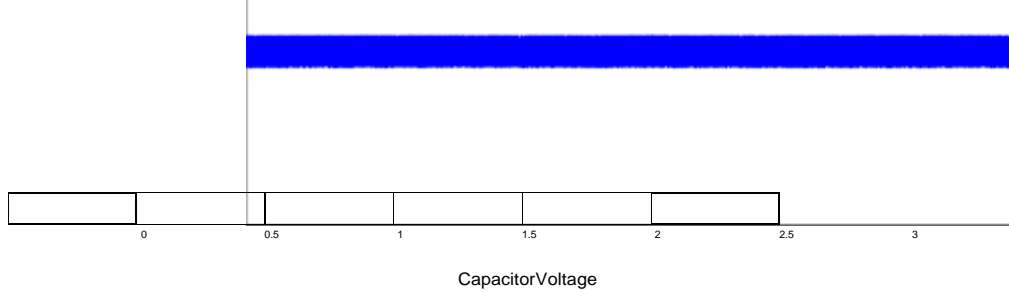


Figure12.Outputwaveformofcapacitorcurrent

Theabovefigureshowsoutputwaveformofcapacitorcurrent.InthisX-

axisrepresentstimeinsecondsandY-axisrepresentscapacitorcurrentinamperes.

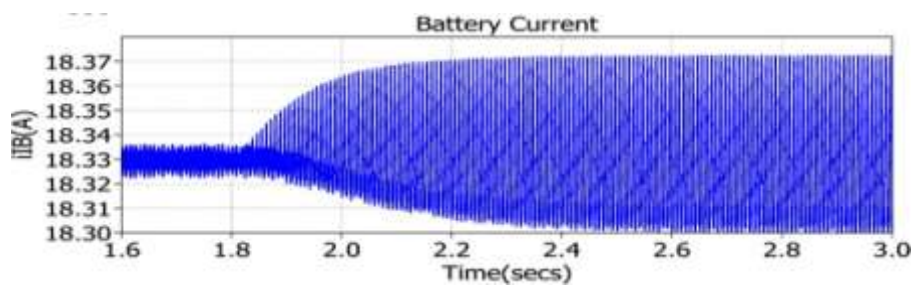


Figure13.Outputwaveformofbatterycurrent

Theabovefigureshowsoutputwaveformofbatterycurrent.InthisX-axisrepresentstimeinsecondsandY-axisrepresentsbatterycurrentinamperes.

Figure14.OutputwaveformPVpower

TheabovefigureshowsoutputwaveformofPVpower.InthisX-axisrepresentstimeinsecondsandY-axisrepresentspowerinwatts.

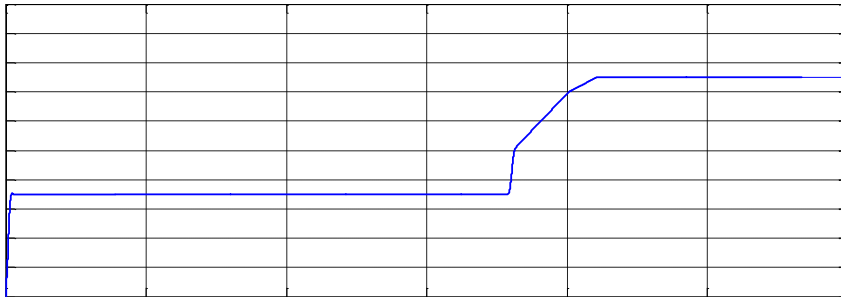
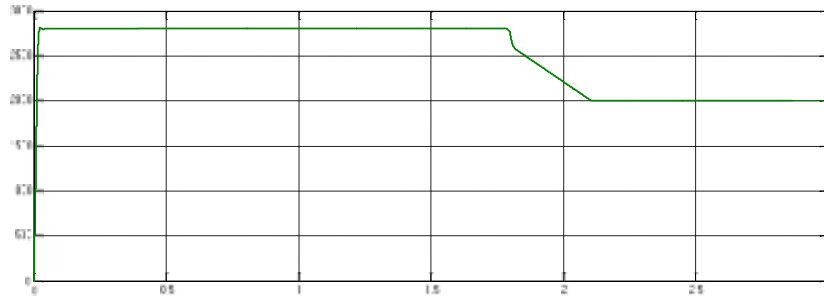


Figure15.OutputwaveformofGridPower

Theabovefigureshowsoutputwaveformofgridpower.InthisX-axisrepresentstimeinsecondsandY-axisrepresentsgridpowerinwatts.

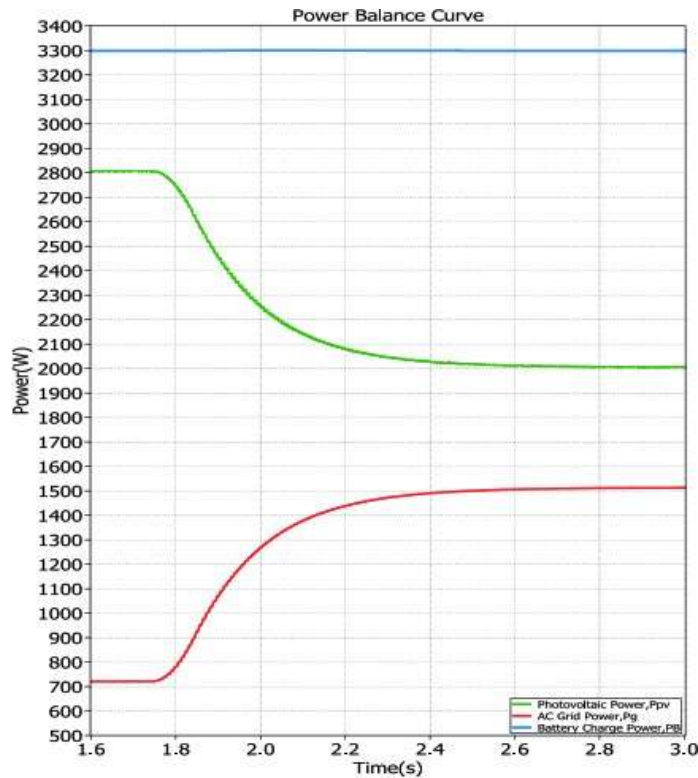


Figure 16. Simulation waveform for the power balance between the PV input power, the ac grid side, and the battery power

7

Conclusion

For PV-grid-connected charging systems, this article recommends a MZSI structure. For charging or energy storage, it has a single-stage PV-grid connection and an integrated charger. In semi-commercial settings like a shopping center parking lot, this topology can be employed in clustered charging configurations. When using string inverters for residential use, the charger side can be connected in series or parallel for current sharing. A Z-source converter's impedance network can be used to create a symmetrical

energy storage topology, according to this paper.

REFERENCES

Aggeler, D.; Canales, F.; Zelaya-De La Parra, H.; Coccia, A.; However, N.; and Apeldoorn, O. (2010, October). Electric vehicles and future smart grids will benefit from ultra-fast DC charging facilities. An ISGT Europe was held in 2010 during the IEEE PES Innovative Smart Grid Technologies Conference (pp. 1-8). IEEE.

2 Carli, G., & S. S. Williamson [2] (2013). Photovoltaic battery charging in electric and

plug-in hybrid electric vehicles: technical issues for power conversion. Applied electrical engineering, 28(12), 5784-5792.

[1] Ingersoll, J.G., & Perkins, C.A. (1996, May). The 2.1 kW photovoltaic electric vehicle charging station in the city of Santa Monica, California. In Conference Record of the Twenty-Fifth IEEE Photovoltaic Specialists Conference-1996 (pp. 1509-1512). IEEE.

[2] Bai, S., Yu, D., & Lukic, S. (2010, September). Optimum design of an EV/PHEV charging station with DC bus and storage system. In 2010 IEEE Energy Conversion Congress and Exposition (pp. 1178-1184). IEEE.

[3] Ninad, N.A., & Lopes, L.A. (2007, October). Operation of single-phase grid-connected inverters with large DC bus voltage ripple. In 2007 IEEE Canada Electrical Power Conference (pp. 172-176). IEEE.

[4] Araújo, S.V., Zacharias, P., & Mallwitz, R. (2009). Highly efficient single-phase transformerless inverters for grid-connected photovoltaic systems. IEEE Transactions on Industrial Electronics, 57(9), 3118-3128.

[5] Meneses, D., Blaabjerg, F., Garcia, O., & Cobos, J.A. (2012). Review and comparison of step-up transformerless topologies for photovoltaic AC-module application. IEEE Transactions on Power Electronics, 28(6), 2649-2663.

[6] D. Meneses, F. Blaabjerg, O. García, and J. A. Cobos, —Review and comparison of step-up transformerless topologies for photovoltaic module application, IEEE Trans. Power Electron., vol. 28, no. 6, pp. 2649–2663, Jun. 2013.

[7] González, R., Lopez, J., Sanchis, P., & Marroyo, L. (2007). Transformerless inverter for single-phase photovoltaic systems. IEEE Transactions on Power Electronics, 22(2), 693-697.

[8] Kjaer, S.B., Pedersen, J.K., & Blaabjerg, F. (2005). A review of single-phase grid-connected inverters for photovoltaic modules. IEEE transactions on industry applications, 41(5), 1292-1306.

Author's Profile:



PESALAVENKATAPRAVEENKUMAR, completed B.Tech in Electrical and Electronics Engineering in 2017 from Dr. Samuel George Institute of Engineering and Technologies affiliated to JNTU Kakinada and pursuing M. Tech from Dr Samuel George Institute of Engineering and Technology affiliated to JNTU Kakinada,

Andhra Pradesh, India. Area of interest including Power electronics, Recent Technologies in Electric Vehicles. E-mailid: pravinkumar261996@gmail.com



He is pursuing a PhD in electrical engineering at KL University, Guntur, after completing a bachelor's degree in mechanical engineering at SVH College of Engineering, Machilipatnam. Currently, he is working on his master's degree in power electronics at VRD&YRN College of engineering and technology, which is affiliated to JNTUK. Dr. Samuel George Institute of Engineering & Technology, Markapur, A. P. and India as an associate professor. As a teacher, I have 15 years of experience, and my interests include power converters, integrated systems, and renewable energy. spandu625@gmail.com is my email address.